ELSEVIER

Chemical Engineering Journal 128 (2007) 1–10

Chemical Engineering Journal

www.elsevier.com/locate/cej

Diffusion controlled reaction rate, survival probability, and molecular trajectory characteristics in the bulk, transition and Knudsen regime

Manolis M. Tomadakis *, Deepti Rupani

Department of Chemical Engineering, Florida Institute of Technology, Melbourne, Florida 32901-6975, United States

Received 6 March 2006; received in revised form 1 September 2006; accepted 3 October 2006

Abstract

Random walk simulation results are presented for the diffusion controlled reaction rate coefficient, molecular survival probability, average track length and relative collision frequency in the bulk, transition and Knudsen diffusion regime, in porous media formed by randomly oriented cylindrical fibers. The survival probability and mean survival distance are found to increase with the porosity in all diffusion regimes. The diffusion controlled reaction rate coefficient attains higher values at lower porosities, obeying an upper bound of the literature and approaching its value in the bulk regime. The values computed for all three parameters in the transition regime depend strongly on the Knudsen number, whereas in the Knudsen regime they are in line with analytical predictions based on the chord length distribution of the fiber structures. A harmonic average approximation based on Bosanquet's equation for the effective diffusivities is found to link successfully the values of the diffusion controlled reaction rate coefficient in the three diffusion regimes. The simulation results for the average molecular track length and relative collision frequency deviate in the biggest part of the transition regime from earlier analytical and numerical results obtained from long diffusion time random walks, in agreement with an analysis centered on the basic differences of molecular trajectories in diffusion controlled reaction systems from those involving molecular reflection from the pore surface.

Keywords: Diffusion controlled reaction; Rate coefficient; Bulk, transition and Knudsen regime; Survival probability; Collision frequency; Track length; Fibrous porous media; Random walks

1. Introduction

Porous media formed by random arrays of fibers are encountered in a variety of modern technology applications, including hydrogen fuel cells, fibrous filters and membranes, paper products, thermal insulations, physiological systems and processes, and fiber-reinforced composites used extensively in the aerospace and automobile industry. In the recent past, Tomadakis and Sotirchos [1,2] investigated bulk, transition, and Knudsen regime diffusion through various types of random fiber structures involved in these applications. The authors emphasized the significance of mass transport and heterogeneous reaction in all diffusion regimes in the above systems, and investigated the relative contribution of molecule-wall and intermolecular collisions to the corresponding mass transfer resistance. The Bosanquet formula, predicting the transition regime effective diffusivity as the harmonic average of the bulk and Knudsen diffusivities, was validated for diffusion in complex porous environments [1–3], justifying its use in mathematical models of transport and reaction in such media.

Diffusion controlled heterogeneous reactions arise in a number of industrial and other applications, including coal gasification [4], char combustion [5], gas desulfurization [6], syn-gas production [7], fiber-reinforced composite manufacturing [8], and cell chemoreception [9]. The corresponding effective reaction rate coefficient is determined by the time scale of molecular transport to the pore surface, hence it relates directly to the molecular survival probability [10–13], representing the fraction of molecules that do not reach that surface up to a given time into the process. This cumulative probability distribution, as well as the average of the corresponding probability density, the mean survival time, are integral also to other processes involving transport in multiphase environments, such as the magnetization decay in nuclear magnetic resonance [14], and the viscous flow through beds of particles and porous media [15–17]. Most investigations of the diffusion controlled reac-

* Corresponding author. Tel.: +1 321 674 7243; fax: +1 321 674 7565.
E-mail address: tomadaki@fit.edu (M.M. Tomadakis).

1385-8947/$ – see front matter © 2006 Elsevier B.V. All rights reserved.
doi:10.1016/j.cej.2006.10.005

tion rate coefficient, survival probability and mean survival time in porous environments focused on the bulk diffusion regime, where intermolecular collisions are the dominant source of mass transfer resistance. An exemption to that is the study by Levitz [18], who presented both analytical and numerical results for the Knudsen regime survival probability in a dense random packing of hard spheres, and encountered good agreement between the two sets of predictions. To our knowledge, no study has been reported to date on the variation of any of the above parameters in the transition diffusion regime, for any type of porous medium.

The track length distributions and collision frequencies associated with the transport of particles in the proximity of solid surfaces have attracted research interest in diverse fields such as acoustics, nuclear reactor design, cosmic ray dosimetry in the natural environment, and radiation dosimetry in biological systems and microelectronics ([19] and references therein). The bulk of these studies examined the characteristics of random chords, i.e., tracks with both ends on the surface of a solid body, and only a few looked into random tracks with one or both ends in the interior of the body. Such tracks and the events they stand for are almost always important, if not dominant, especially in applications involving heavy-particle recoils, as shown by Caswell [20] in his study of neutron dosimetry. The author identified four types of recoil interaction with cavities, and described the corresponding tracks using the following terms: insiders (paths that are completed within the body, without interfering with the surface), crossers (paths with both ends on the solid surface, i.e., chords), and starters and stoppers (paths with one end on the surface and the other in the interior of the body). The same terminology was adopted by Kellerer [21] in a probabilistic analysis of random paths in objects of arbitrary shape, and by Tomadakis and Sotirchos [1,19] in their analytical and numerical investigations of mass transport in random arrays of cylindrical fibers and capillaries. No literature study has looked yet into the characteristics of such distinct types of tracks, or the corresponding overall track length distribution and collision frequency, in systems exhibiting a negligible frequency of molecular reflection from the solid surface, i.e., systems associated with diffusion controlled reactions, or, more generally, perfectly absorbing walls.

The purpose of the present study is to compute the diffusion controlled reaction rate constant, survival probability, relative collision frequency, average track length, and average size of insiders and stoppers in randomly oriented fiber structures, in the bulk, transition and Knudsen diffusion regime, throughout the porosity range. In Section 2, we outline the basic theoretical principles and methods involved in this work, and present analytical results for the Knudsen regime survival probability and diffusion controlled reaction rate coefficient, derived from probabilistic relations of the literature. In Section 3, we present our numerical results for all investigated parameters, and compare them to the analytical predictions of Section 2, an upper bound of the literature, and earlier numerical and analytical results for the relative collision frequency, average track length, and average size of insiders and stoppers. In the same section, we introduce a harmonic average approximation for the diffusion controlled reaction rate constant, and compare its predictions to our simulation results in the three diffusion regimes. Our main conclusions are summarized in Section 4.

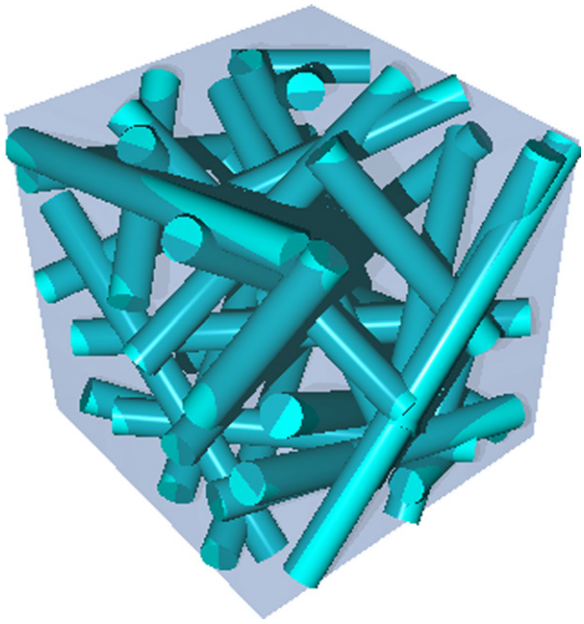

Fig. 1. Illustration of the fiber orientation distribution in 3-d random fiber structures.

2. Theoretical principles and methods

2.1. Fiber structures and diffusion regimes

The fiber structures investigated in this study consist of freely overlapping cylindrical fibers with axes oriented randomly in the three-dimensional space (3-d random fiber structures), as shown in a schematic illustration in Fig. 1. Numerical samples of such porous media are generated with the "μ-randomness" construction mechanism, the only such mechanism that produces statistically isotropic and homogeneous samples of random beds of fibers [22]. According to this construction technique, the fiber axes are obtained as μ-random lines, i.e., lines defined by a point on a fixed plane and a direction with respect to that plane, with the point obtained randomly from a uniform distribution and the direction independently, from a properly defined and bounded probability measure [1,22]. The mean intercept length ($\bar{d}$) of such random arrays of fibers (i.e., the average track length of molecules undergoing Knudsen diffusion in the porous channels of the structure – a characteristic pore size of the porous medium), relates to the bed porosity, ε, and the fiber radius, r, through [23]

$$\bar{d} = \frac{-2r}{\ln \varepsilon} \tag{1}$$

The corresponding average track length in the bulk diffusion regime is the "mean free path" $\bar{\lambda}$, related to the mean molecular diameter and concentration (hence pressure and temperature) by the kinetic theory of gases. The relative value of these two parameters is the Knudsen number ($\mathrm{Kn} = \bar{\lambda}/\bar{d}$), commonly used

to parameterize the diffusion process in porous environments. For $Kn \leq 0.02$, diffusion occurs in the ordinary (bulk) diffusion regime, characterized by high molecular concentration and intermolecular collision frequency. At the other end of the diffusion spectrum, for $Kn \geq 100$, molecule–molecule collisions are rare due to the low gas density, and Knudsen diffusion is the dominant mode of mass transport. For $0.02 < Kn < 100$, both intermolecular and molecule-wall collisions contribute significantly to the mass transfer resistance, i.e., transition regime diffusion conditions prevail. The critical values of the Knudsen number (0.02, 100) were determined in an earlier investigation of diffusion in fiber structures [1], based on the values of the tortuosity factor throughout the Kn range, and were instrumental in the validation of the harmonic average approximation and other analytical predictions and variational bounds of the literature [1].

Typical values of the fiber radius (r) in applications range from 1 to about 100 μm. For the porosity range investigated in this study ($\varepsilon = 0.1$–0.99), Eq. (1) predicts an equivalent characteristic pore size ($\bar{d}$) ranging from 0.9 μm to about 1 cm. This is orders of magnitude higher than the size of diffusing molecules, practically eliminating steric effects induced by space constraints that would invalidate the use of mathematical points (random walkers) to depict fluid molecules in our simulation algorithms (Section 2.4).

2.2. Diffusion controlled reaction rate and survival probability

Let us consider a process where a solute diffuses in the void space of a porous medium and is consumed by heterogeneous reaction on the pore surface. When the pseudo-homogeneous hypothesis is used to model this mass transport and reaction problem, volume averages for the solute concentration, C_A, and net production rate, R_A, are typically obtained from

$$\hat{C}_A = \frac{1}{V}\int_{V_p} C_A \mathrm{d}V; \tag{2a}$$

$$\hat{R}_A = \frac{1}{V}\int_{S_p} R_A \mathrm{d}S \tag{2b}$$

where V is the volume of the porous medium, V_p the pore volume, and S_p the pore surface. $\hat{R}_A$ is conveniently related to $\hat{C}_A$ through an effective first-order reaction rate constant, k

$$\hat{R}_A = -k\hat{C}_A \tag{3}$$

At the continuum (bulk) level, this relation is obtained directly from the method of volume averaging, where the pseudo-homogeneous reaction rate constant, k, is expressed in terms of other rigorously defined structure and reaction coefficients [24]. When an "intrinsic volume average" $\hat{C}_{A,p} = \frac{1}{V_p}\int_{V_p} C_A \mathrm{d}V$ is used in place of $\hat{C}_A$ [24], Eq. (3) readily becomes $\hat{R}_A = -k_p\hat{C}_{A,p} = -k\varepsilon\hat{C}_{A,p}$ (since $\hat{C}_A/\hat{C}_{A,p} = V_p/V = \varepsilon$).

When the rate of the surface reaction is very fast compared to that of mass transport to the surface (i.e., when diffusion controlled reaction conditions prevail), the value of k is determined exclusively by the time scale of molecular transport to the pore surface, and may be obtained directly from the corresponding survival probability, $S(t)$ [10,14]

$$k^{-1} = \tau = \int_0^\infty S(t)\mathrm{d}t \tag{4}$$

where τ is the mean survival time, i.e., the average time taken by the diffusing molecules before colliding and reacting instantaneously on the pore surface. Eq. (4) has been used in random walk investigations for the estimation of the effective reaction rate constant k for Brownian (bulk) diffusion in beds of spheres [11,13] and spheroids [12]. It should be noted that the k values derived in the context of Eq. (4) are limited by the time constraint $t \gg \tau$, i.e., they are applicable in processes where able time is allowed for the diffusing molecules to probe the pore surface geometry. The constraint is satisfied in most applications, since typical values of the mean survival time are $\tau \ll 1$ s (e.g., case example in Table 2, Section 3.2).

The pore geometry effect on k and τ enters through an entirely structure-dependent parameter, namely, the dimensionless survival distance, s/r, representing the total path length until a molecule reacts on the pore surface. The mean survival time, τ, relates to the mean survival distance, $\bar{s}$, and the mean thermal speed, $\bar{v}$, through $\tau = \bar{s}/\bar{v}$. It may be rendered dimensionless using a reference diffusivity D_p, defined as the self-diffusion coefficient of the gas in a cylindrical pore of diameter equal to the mean intercept length of the fibrous structure ($\bar{d}$) under the same pressure and temperature (the same continuum mean free path $\bar{\lambda}$) as in the porous medium. D_p is known to follow the harmonic average relation proposed by Bosanquet (Pollard and Present [25]).

$$\frac{1}{D_p} = \frac{1}{D_b} + \frac{1}{D_K} \tag{5}$$

where D_b is the bulk self-diffusion coefficient, which for a no-memory random walk is given by $D_b = 1/3\bar{v}\bar{\lambda}$, and D_K is the Knudsen diffusivity in a pore of diameter $\bar{d}$: $D_K = 1/3\bar{v}\bar{d}$. Substituting these expressions into Eq. (5) along with the definition of the Knudsen number ($Kn = \bar{\lambda}/\bar{d}$), we obtain

$$D_p = \frac{D_b}{1 + Kn} = \frac{D_K}{1 + Kn^{-1}} \tag{6}$$

It is evident from Eq. (6) that the reference diffusivity, D_p, becomes practically equal to D_b in the bulk diffusion regime ($Kn \ll 1$) and to D_K in the Knudsen regime ($Kn \gg 1$). Combining Eq. (6) with Eq. (1) and $D_K = 1/3\bar{v}\bar{d}$, $k^{-1} = \tau = \bar{s}/\bar{v}$, we derive

$$\left(\frac{kr^2}{D_p}\right)^{-1} = \frac{\tau D_p}{r^2} = \frac{-2(\bar{s}/r)}{3\ln\varepsilon}\left(\frac{1}{1 + Kn^{-1}}\right) \tag{7}$$

Once the dimensionless mean survival distance, $\bar{s}/r$, is obtained from the random walks at a given porosity and Knudsen number, Eq. (7) allows for a straightforward conversion to the corresponding dimensionless mean survival time, $\tau D_p/r^2$, and effective reaction rate constant, kr^2/D_p.

2.2.1. Analytical derivations in the Knudsen regime

The chord length probability density, $P_\mu(d)$, is defined as the fraction of chords of length d, out of all possible chords formed by the traversal of a body by μ-random lines. Such secants have size and orientation distributions identical to those of actual tracks of molecules diffusing in the void space of the medium in the Knudsen regime [1]. Consequently, μ-random chord segments that originate in the void space and end on the surface of the body provide a reliable model for the one-step molecular survival distances in that regime of diffusion. The distribution density of such chord segments may be readily obtained from a probabilistic analysis in the form [18]

$$P(s) = \frac{1}{\bar{d}} \int_s^\infty P_\mu(d')dd' \tag{8}$$

The corresponding complementary cumulative distribution function, $F(s) = \int_s^\infty P(s)\mathrm{d}s$, is equivalent to a distance-based survival probability distribution in the Knudsen regime, as it stands for the fraction of molecules with survival distance higher than s

$$F(s) = \frac{1}{\bar{d}} \int_s^\infty \int_{s'}^\infty P_\mu(d')dd'ds' \tag{9}$$

Eq. (9) may be used to derive $F(s)$ for any type of porous medium of known chord length probability density, $P_\mu(d)$. Tomadakis and Sotirchos [1] offered analytical predictions for $P_\mu(d)$ in random fiber structures of various directionalities, and validated their theoretical results through random walk simulations. For the isotropic 3-d random fiber structures, their prediction is a simple exponential distribution of the form

$$P_\mu(d) = \frac{1}{\bar{d}} \exp\left(-\frac{d}{\bar{d}}\right) \tag{10}$$

which may be substituted into Eq. (9) to give readily

$$F(s) = \mathrm{e}^{-s/\bar{d}} \tag{11}$$

This complementary cumulative distribution function may be expressed in terms of ε and r using Eq. (1), then readily converted to the corresponding time-based survival probability $S(t)$ using Eq. (7) [written for an arbitrary set of s, t values (instead of the mean values $\bar{s}$, τ) and simplified for Knudsen diffusion (Kn ≫ 1): $tD_\mathrm{p}/r^2 = -2(s/r)/3\ln\varepsilon$]. The resulting analytical prediction for the Knudsen regime survival probability distribution in 3-d random fiber structures is

$$S(t) = \exp\left(-0.75\ln^2\varepsilon\left(\frac{tD_\mathrm{p}}{r^2}\right)\right) \tag{12}$$

The chord length probability density of 3-d random arrays of fibers (Eq. (10)) may be substituted directly into Eq. (8) to give

$$P(s) = \frac{1}{\bar{d}}\mathrm{e}^{-s/\bar{d}} = P_\mu(s) \tag{13}$$

Evidently, the probability distribution of chord segment lengths is identical with the chord length probability distribution for isotropic (μ-random) fields in 3-d random fiber structures. Equal values are predicted therefore for the means of the two probability densities, namely, the mean survival distance and the mean intercept length: $\bar{s} = \int_0^\infty F(s)\mathrm{d}s = \int_0^\infty e^{-s/\bar{d}}ds = \bar{d}$. The corresponding dimensionless mean survival distance is readily obtained using also Eq. (1):

$$\frac{\bar{s}}{r} = \frac{\bar{d}}{r} = \frac{-2}{\ln\varepsilon} \tag{14}$$

The diffusion controlled reaction rate constant and the mean survival time for Knudsen diffusion in 3-d random arrays of fibers are obtained from Eqs. (4) and (12) as $k^{-1} = \tau = 4r^2/(3\ln^2\varepsilon D_\mathrm{p})$, or in dimensionless form

$$\left(\frac{kr^2}{D_\mathrm{p}}\right)^{-1} = \frac{\tau D_\mathrm{p}}{r^2} = \frac{4}{3\ln^2\varepsilon} \tag{15}$$

The predictions of Eqs. (12), (14) and (15) are compared to the outcome of our random walk simulations in Section 3.

2.3. Average track length and relative collision frequency

Tomadakis and Sotirchos [1] derived theoretical expressions for the relative collision frequency and average size of tracks for diffusion in random fiber structures, and validated their predictions through random walks. For the dimensionless mean track length, l_a (i.e., the average size of all molecular steps in the diffusion trajectories), they predicted $1/l_\mathrm{a} = 1/\bar{\lambda} + 1/\bar{d}$, i.e.,

$$\frac{l_\mathrm{a}}{\bar{\lambda}} = \frac{1}{1+\mathrm{Kn}} \tag{16}$$

This expression was first derived by Bosanquet (Pollard and Present [25]) for diffusion in a cylindrical tube, but was shown by the authors [1] to be valid also for more complex porous media, of either isotropic or anisotropic nature. For the corresponding relative frequency of molecule-wall to intermolecular collisions, they derived and validated numerically the relation

$$\frac{C_\mathrm{w}}{C_\mathrm{m}} = \mathrm{Kn} \tag{17}$$

They also showed analytically and through random walks that, for diffusion in the isotropic 3-d random fiber structures, the average length of insiders, l_i, is equal to the average length of stoppers, l_s, and to the overall average track length, l_a

$$l_\mathrm{i} = l_\mathrm{s} = l_\mathrm{a} \tag{18}$$

The predictions of Eqs. (16)–(18) are compared in the next section to our simulation results derived from diffusion controlled reaction trajectories in 3-d random arrays of fibers.

2.4. Random walk simulation technique

The simulations are carried out using an earlier random walk algorithm [1] modified to account for molecular trajectory termination at first impact with the solid surface. A unit cubic cell is created first as outlined in Section 2.1, to represent numerically the fiber structure. A random position is generated next within the unit cell; if it falls in the void space it becomes the starting position for a random walk. Random direction cosines are assigned to the walker, and a molecular free path λ is sampled

from an exponential distribution of mean equal to $\bar{\lambda} = \mathrm{Kn}\,\bar{d}$. Before the molecule can be moved to that point, verification is made that it will not encounter a fiber or cell boundary within that distance. As long as no such interference is encountered, the above procedure is repeatedly applied to simulate a sequence of intermolecular collisions. If one or more fibers are found to lie within the path of the advancing molecule, the shortest distance between the origin of this step and the fibers determines the next position of the walker. In diffusion controlled reaction systems, the solute is consumed instantaneously on the pore surface, therefore no reflection of the walker from the solid surface is accounted for, and the simulation continues by placing the next random walker in the unit cell. The procedure is complete when a total of 10,000 random walks are performed at each porosity level, for every selected value of the Knudsen number.

When a random walker reaches the boundary of the cubic cell, it is specularly reflected on it and returned to the cell. This is equivalent to treating the porous medium as an infinite assemblage of identical unit cells, with each neighboring cell being a mirror image of the next. The use of such boundary conditions does not introduce any measurable bias in the simulation results, provided that a big enough sample of the random fiber structure is investigated, i.e., a high enough population of fibers is present in the unit cell [1]. Trajectory computations are accelerated considerably by using time-saving modifications of the basic algorithm, namely, a spherical inclusion technique exploiting the basic idea of first-passage-time random walks, and certain domain and path discretization schemes [1].

Keeping track of the total length of the random walker trajectories, as well as the number and length of all encountered insiders and stoppers, enables the derivation of the survival probability distribution, mean survival distance, average track lengths and collision frequencies for the investigated fiber structures, for a broad range of porosities and Knudsen numbers.

Direct simulation Monte Carlo techniques, such as the one described above, are known to simulate successfully the basic characteristics of actual molecular movements when they employ accurate enough, experimentally validated probabilistic models for the involved microscopic phenomena (such as distributions of free paths between intermolecular collisions, distributions of reflection angles following intermolecular or molecule-wall collisions, etc.) [1]. The outcome of such studies is in line with experimental measurements [1,26], as well as with the results of molecular dynamics simulations (which account explicitly for all involved phenomena, tracking simultaneously the movements and interactions of thousands of molecules, at a nearly prohibitive computational cost).

3. Results and discussion

3.1. Survival probability

Survival probability distribution curves obtained from our simulations for various values of the Knudsen number at $\varepsilon = 0.1$, 0.5, and 0.99 are shown in Figs. 2–4, respectively. Since $S(t)$ is a complementary cumulative distribution function, all curves in

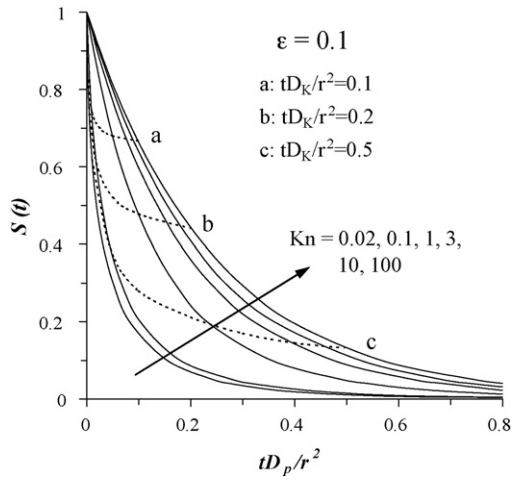

Fig. 2. Variation of the survival probability distribution with the Knudsen number at $\varepsilon = 0.1$.

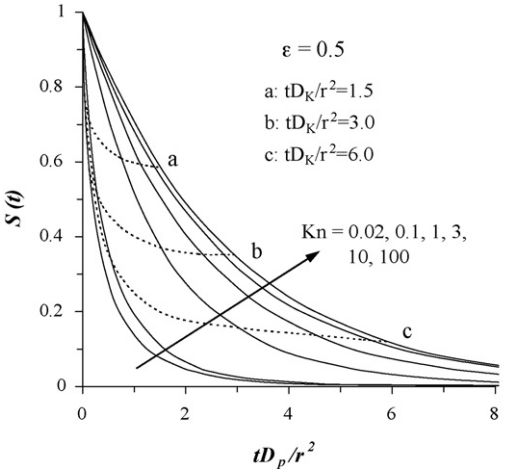

Fig. 3. Variation of the survival probability distribution with the Knudsen number at $\varepsilon = 0.5$.

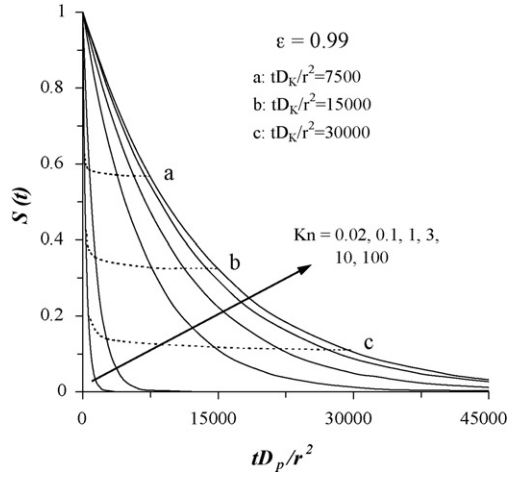

Fig. 4. Variation of the survival probability distribution with the Knudsen number at $\varepsilon = 0.99$.

these plots originate at point (0, 1) and extend asymptotically to zero at very high survival times. For a given gas species, pressure, temperature, structural properties (ε, r), and time, both Kn and tD_p/r^2 are uniquely defined and can be used readily in Figs. 2–4 to obtain the respective value of the survival probability. Nonetheless, the value of the dimensionless survival time, tD_p/r^2, is determined in part by Kn, through the reference diffusivity D_p (Eq. (6)). As a result, the effect of Kn on $S(t)$ at a constant diffusion time, t, is not readily deduced by visual inspection of the basic (solid) curves of these plots. For that reason, curves of constant tD_K/r^2 are also plotted in the figures, obtained straightforwardly from $tD_K/r^2 = tD_p/r^2(1 + Kn^{-1})$ (i.e., Eq. (6)). These curves become lines of constant t when the Knudsen number is varied in the most simple and practically meaningful manner, i.e., by manipulating the value of the molecular mean free path through pressure variation (thereby keeping the value of D_K constant). Moving along any such curve in the direction of increasing Kn, we encounter a decreasing survival probability $S(t)$. This obviously means that a higher fraction of molecules collides with the wall by a certain time t for a higher Knudsen number (i.e., when fewer molecules are present in a certain volume), as anticipated by intuition. The effect is less pronounced in the dilute limit (Fig. 4), where the survival probability is determined primarily by the very high value of the mean intercept length, for all but the highest gas densities (Kn > 0.1).

It is evident by comparison of Figs. 2–4 that higher survival times are reached at higher porosities for the same Knudsen number. This is anticipated intuitively too, since bigger voids are present in high porosity structures, allowing for longer diffusion times before collision with the pore surface. The effect is by far more pronounced in the dilute limit (Fig. 4), where collisions of molecules with the solid wall become very scarce. A closer look at the porosity effect on the survival probability in the transition and Knudsen regime is offered in Figs. 5–7, where $S(t)$ is plotted for various porosities at two fixed values of Kn, namely Kn = 1 and 100. The analytical prediction for the Knudsen regime survival probability (Eq. (12)) is also plotted in Figs. 6–7, and is found to be in excellent agreement with our numerical results for Kn = 100, at all porosity levels. To assess

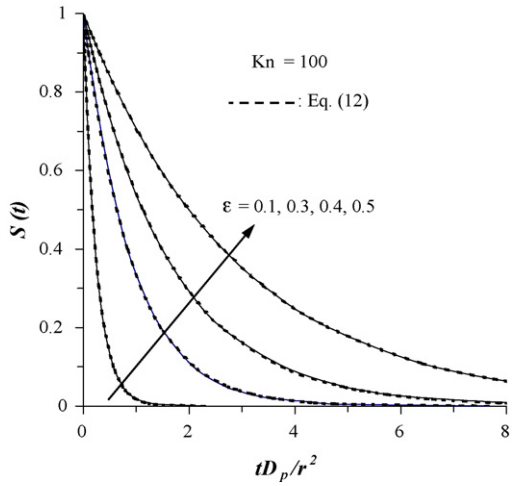

Fig. 6. Variation of the survival probability distribution at low porosities and Kn = 100.

the effect of the number of random walkers on the accuracy of the simulation results, the random walks for Kn = 1 and $\varepsilon = 0.50$ were carried out using five different sets of 10,000 random walkers, and the tD_p/r^2 values derived for each set at fixed values of the survival probability, $S(t)$, were compared to the corresponding average values obtained at the same $S(t)$ for all five sets of walkers. For survival probabilities higher than 0.01, the value of tD_p/r^2 obtained for each set was found to deviate from the corresponding average value by a mere 1–2.7%, revealing a negligible effect of the number of employed random walkers on the simulation results, for all practical purposes.

Our numerical results for the dimensionless mean survival distance, $\bar{s}/r$, are presented in Fig. 8 (data markers), plotted against the Knudsen number for various values of the porosity. As is evident in this plot, lower values of the mean survival distance are encountered in the upper transition and Knudsen regime, due to the significantly lower number of intermolecular collisions associated with this type of diffusion. At the right end of the diffusion spectrum (Kn ≥ 100), the mean survival distance

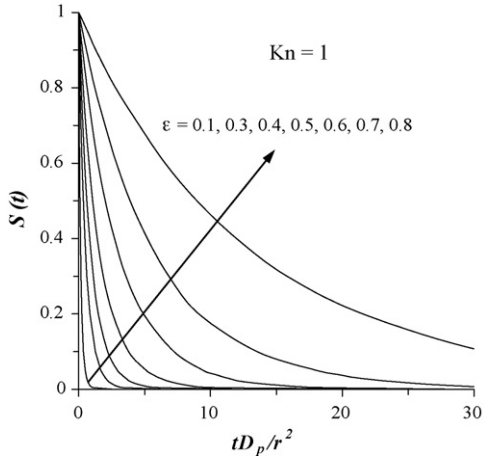

Fig. 5. Variation of the survival probability distribution with the porosity at Kn = 1.

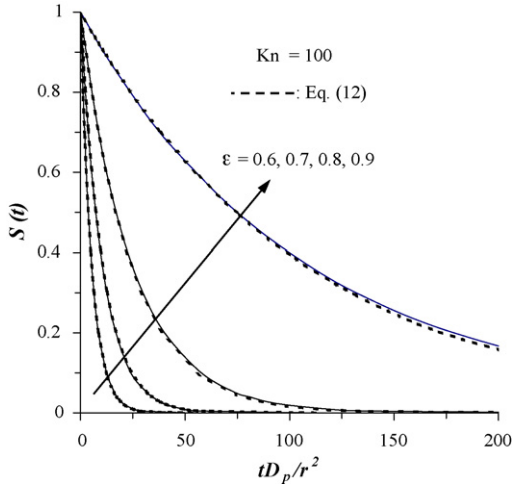

Fig. 7. Variation of the survival probability distribution at high porosities and Kn = 100.

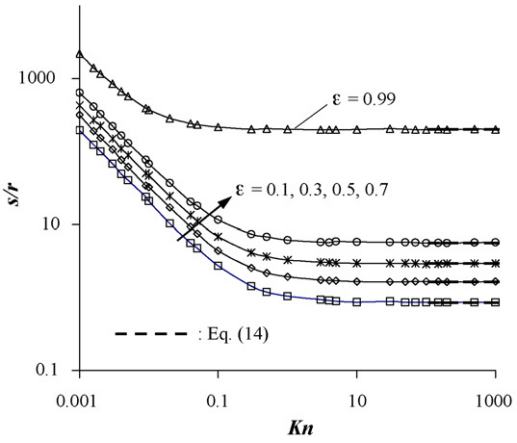

Fig. 8. Variation of the mean survival distance with the Knudsen number at various porosities.

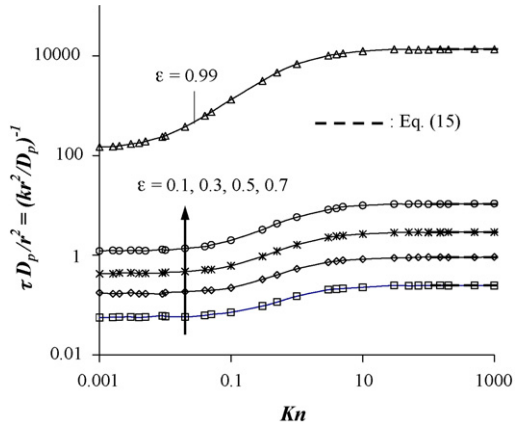

Fig. 9. Variation of the diffusion controlled reaction rate coefficient and mean survival time with the Knudsen number at various porosities.

evens out to the value predicted by Eq. (14) for each value of the porosity. In the dilute limit ($\varepsilon = 0.99$), the agreement of Eq. (14) with our numerical data extends to Knudsen numbers as low as 0.1, in line with the observations made earlier for the survival probability (Fig. 4). Naturally, in the lower transition and bulk regime, the dimensionless mean survival distance attains higher values; the linearity of the log–log curves in the bulk regime indicates that the numerical results follow the simple inverse proportionality relation $\bar{s}/r = c/\mathrm{Kn}$, with the value of the constant c linked to that of the diffusion controlled reaction rate constant, as outlined in the following paragraph.

3.2. Diffusion controlled reaction rate coefficient

Fig. 9 presents the variation of the dimensionless diffusion controlled reaction rate coefficient, kr^2/D_p, and mean survival time, $\tau D_\mathrm{p}/r^2$, with the Knudsen number, throughout the porosity range. In the bulk diffusion regime, the two dimensionless groups remain practically constant and equal to the values reported by Tomadakis and Robertson [26] for each porosity level. This behavior is in line with the above made observation that the dimensionless survival distance varies in inverse proportionality to the Knudsen number in the bulk regime (where $(kr^2/D_\mathrm{b})^{-1} = \tau D_\mathrm{b}/r^2 = -2Kn(\bar{s}/r)/3\ln\varepsilon$, as deduced from Eq. (7) for $\mathrm{Kn} \ll 1$). In the transition regime, the two dimensionless numbers vary with Kn, and even out in the Knudsen regime to the values predicted analytically (Eq. (15)). The shape of the numerically derived curves in Fig. 9 prompts us to postulate that the simulation results in the three diffusion regimes may be linked through

$$k_\mathrm{d}^{-1} = \frac{k_\mathrm{b,d}^{-1} + \mathrm{Kn}\, k_\mathrm{K,d}^{-1}}{1 + \mathrm{Kn}} \tag{19}$$

where k_d stands for the dimensionless diffusion controlled reaction rate constant ($k_\mathrm{d} = kr^2/D_\mathrm{p}$) and $k_\mathrm{b,d}$, $k_\mathrm{K,d}$ for its limiting values in the bulk and Knudsen diffusion regime ($k_\mathrm{d} \to k_\mathrm{b,d}$ as $\mathrm{Kn} \to 0$, and $k_\mathrm{d} \to k_\mathrm{K,d}$ as $\mathrm{Kn} \to \infty$). Eq. (19) is of similar form to one shown by Tomadakis and Sotirchos [1] to link rigorously the tortuosity coefficients in the three diffusion regimes in random isotropic fiber structures, thereby leading to the numerical validation of the Bosanquet harmonic average approximation for the effective diffusivities in such porous media. Table 1 presents the outcome of a statistical analysis aimed at a comparison of the predictions of Eq. (19) with the numerical data of Fig. 9. Specifically, the table presents the average value and standard deviation of the ratio $k_\mathrm{d,Eq.\ (19)}/k_\mathrm{d,simul}$, as well as the average prediction error $\langle |k_\mathrm{d,Eq.\ (19)} - k_\mathrm{d,simul}|/k_\mathrm{d,simul} \rangle$, both for the whole transition regime and separately for its upper and lower parts. As is evident in the table, Eq. (19) provides a very good approximation to the transition regime diffusion controlled reaction rate coefficient, for all practical purposes. Its predictions are particularly accurate in the upper transition regime ($1 < \mathrm{Kn} < 100$), where they deviate from the simulation results by a mere 1% on the average, without systematically over- or under-predicting the numerical data ($\langle k_\mathrm{d,Eq.\ (19)}/k_\mathrm{d,simul} \rangle = 0.997$). It is worth mentioning that the statistical results presented in Table 1 are independent of the porosity, with all reported values remaining practically constant throughout the investigated porosity range ($0.1 \le \varepsilon \le 0.99$).

Substituting back into Eq. (19) the expressions defining Kn, k_d, D_p and their limiting values in the bulk and Knudsen regimes,

Table 1
Comparison of the predictions of Eq. (19) to the random-walk simulation results

Diffusion regime	Knudsen range	$\left\langle \frac{k_\mathrm{d,Eq.(19)}}{k_\mathrm{d,simul}} \right\rangle \pm \sigma$	$\left\langle \frac{\lvert k_\mathrm{d,Eq.(19)} - k_\mathrm{d,simul} \rvert}{k_\mathrm{d,simul}} \right\rangle$
Upper transition	$1 < \mathrm{Kn} < 100$	0.997 ± 0.011	0.010
Lower transition	$0.02 < \mathrm{Kn} \le 1$	0.954 ± 0.021	0.048
Total transition	$0.02 < \mathrm{Kn} < 100$	0.977 ± 0.016	0.027

Table 2
Case example: diffusion and instantaneous surface reaction of hydrogen at 100 mtorr and 1500 K in a random fiber structure of $\varepsilon = 0.5$ and $r = 2\,\mu m$

Kinetic theory: $\bar{\lambda}(P, T, d_{H_2}) = 4.2\,\mu m$; $\bar{v}(T, M_{H_2}) = 4.0\,km/s$
Eq. (1): $\bar{d} = 5.8\,\mu m$; $Kn = \frac{\bar{\lambda}}{\bar{d}} = 0.72$
$D_K = \frac{\bar{v}\bar{d}}{3} = 0.0077\,m^2/s$; $D_b = \frac{\bar{v}\bar{\lambda}}{3} = 0.0056\,m^2/s$;
$D_p = \frac{D_b}{1+Kn} = 0.0033\,m^2/s$
Eq. (15): $k_{K,d} = 0.36$; Figs. 9 and 10: $k_{b,d} = 2.2$
$k_K r^2 = k_{K,d} D_K = 0.0028\,m^2/s$; $k_b r_b^2 = k_{b,d} D_b = 0.0120\,m^2/s$
Eq. (20): $kr^2 = \left(\frac{1}{k_b r_b^2} + \frac{1}{k_K r^2}\right)^{-1} = 0.0023\,m^2/s$
Or, Eq. (19): $k_d = \left(\frac{k_{b,d}^{-1} + Kn k_{K,d}^{-1}}{1+Kn}\right)^{-1} = 0.70$; $kr^2 = k_d D_p = 0.0023\,m^2/s$
$k = \frac{kr^2}{r^2} = 5.8 \times 10^8\,s^{-1}$; $k_K = \frac{k_K r^2}{r^2} = 7 \times 10^8\,s^{-1}$; $[\tau = k^{-1} = 1.7 \times 10^{-9}\,s]$
$k_b(\text{at } r_b = 70\,\mu m) = \frac{k_b r_b^2}{r_b^2} = 2.4 \times 10^6\,s^{-1}$;
$k_b(\text{at } r_b = 200\,\mu m) = \frac{k_b r_b^2}{r_b^2} = 3 \times 10^5\,s^{-1}$

we readily obtain

$$\frac{1}{kr^2} = \frac{1}{k_b r_b^2} + \frac{1}{k_K r^2} \tag{20}$$

This harmonic average approximation links the values of the diffusion controlled reaction rate constant in the three diffusion regimes, much in the same way the Bosanquet equation links the corresponding effective diffusivities [1]. Specifically, k stands for the value of the rate constant at the $\bar{\lambda}$ and $\bar{d}$ of the system, k_K for its value at the system $\bar{d}$ but $\bar{\lambda} \geq 100\bar{d}$, and k_b for its value at the system $\bar{\lambda}$ but $\bar{d} \geq \bar{\lambda}/0.02$ (the latter may be attained only with a high enough fiber radius r_b, as deduced from Eq. (1) and the fact that all terms in Eq. (20) refer to the same porosity). Table 2 presents a case example illustrating the application of the numerical results reported in Figs. 9 and 10 and Eqs. (19) and (20) to systems involving diffusion with instantaneous surface reaction.

Fig. 10 presents the variation of the dimensionless diffusion controlled reaction rate constant, kr^2/D_p, with the porosity, in the bulk ($Kn = 0.02$), transition ($Kn = 1$), and Knudsen ($Kn = 100$) diffusion regime. Lower kr^2/D_p values are attained in the more dilute structures, where bigger voids allow for longer diffusion times before trajectory termination on the pore surface. The numerical results in the Knudsen regime are once again found to coincide with the predictions of Eq. (15). Also plotted in Fig. 10 is an upper bound on the diffusion controlled reaction rate constant in the bulk regime, derived by Prager [27] and evaluated by Strieder [28] for 3-d random fiber structures

$$\frac{kr^2}{D_b} \leq \frac{-4\varepsilon^2 \ln \varepsilon}{\pi(erfc\sqrt{-\ln \varepsilon})^2} \tag{21}$$

The bound is obeyed by our simulation results throughout the porosity range, over-predicting the numerical data in the bulk regime by a small factor of 1.5–2.2 for $\varepsilon \leq 0.9$. This concurs with the observations made by Tomadakis and Robertson [26] on the deviation of the mean survival time in the bulk regime from the corresponding lower bound by Prager [27], evaluated using their numerical results for the mean pore size of the fiber structures.

3.3. Mean track length and relative collision frequency

Our numerical results for the variation of the dimensionless mean track length, $l_a/\bar{\lambda}$, with the Knudsen number for diffusion controlled reaction processes in random fiber structures are plotted in Fig. 11 for various values of the porosity. Also plotted in this figure is the numerically validated analytical prediction of Tomadakis and Sotirchos [1] for mass transfer by diffusion in the same type of porous media (Eq. (16)). As is evident in this plot, our simulation results for the mean track length deviate considerably from those of that study in the lower transition regime ($0.02 < Kn < 1$), but practically coincide at higher and lower Kn, as well as at $\varepsilon \to 1$, throughout the Kn range. The deviation stems from the fact that, in that earlier study [1], the molecular trajectories were not terminated at first impact with the pore sur-

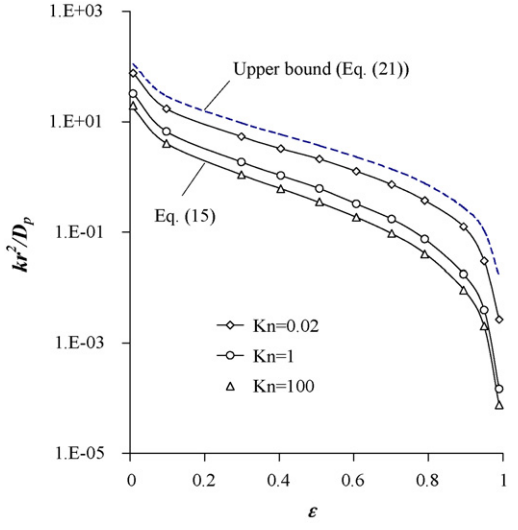

Fig. 10. Variation of the diffusion controlled reaction rate coefficient with the porosity in the bulk, transition, and Knudsen regime.

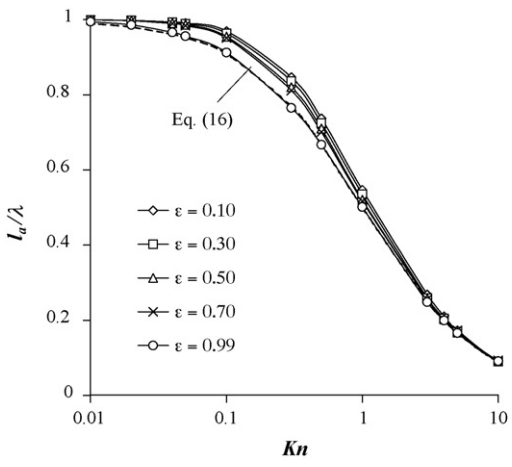

Fig. 11. Variation of the average track length with the Knudsen number at various porosities.

face, but rather continued for a long diffusion distance and time, for the sake of computing the effective diffusivity. As a result, those simulations accounted also for the high number of small paths resulting from wall-to-wall steps inside tiny voids and narrow passages of the porous structure – which are of course not accounted for in this work – thereby leading to smaller values of the overall average molecular track length. In the dilute limit ($\varepsilon \to 1$), formation of such small elements of pore space in the fibrous structures is all but impossible, hence no difference in the predictions of the two studies is expected, in agreement with the trends observed in Fig. 11. The deviations are also eliminated in the bulk diffusion regime, where the probability of encountering wall-to-wall steps is very small, even in such tiny pore volume elements, due to the very small value of the mean free path $\bar{\lambda}$ relative to the mean intercept length $\bar{d}$. The differences are also negligible in the Knudsen and upper transition regime, where the one-step diffusion paths to the pore surface attain distributions and averages identical to those of the μ-random chords employed in the earlier random walks – independently of the existence of small voids in the structure – as discussed in Section 2.2.

Fig. 12 presents our simulation results for the variation of the relative frequency of molecule-wall to intermolecular collisions, C_w/C_m, with the Knudsen number, at various porosities. Since only one collision with the wall is encountered per diffusing molecule in this work, the decreasing values of C_w/C_m at low Kn reflect an increasing intermolecular collision frequency, anticipated intuitively due to the higher gas concentrations attained at low values of the Knudsen number. The observed deviation of our numerical data in the lower transition and bulk regime from the predictions of Eq. (17), as well as the agreement encountered for high values of Kn and for $\varepsilon \to 1$, may be attributed to the same characteristic difference of molecular trajectories in diffusion controlled reaction processes from long diffusion time trajectories, discussed in the previous paragraph. For instance, the low number of molecule-wall collisions in the bulk regime is boosted somewhat in the simulations and theoretical analysis of diffusion in random fiber structures [1], thanks largely to the above mentioned wall-to-wall steps in tiny pore voids and narrow passages, thus maintaining the relative value $C_w/C_m = Kn$, predicted by Eq. (17). In our study of diffusion with instantaneous surface reaction, such wall-to-wall steps are not allowed, thereby keeping the C_w/C_m values at much lower levels.

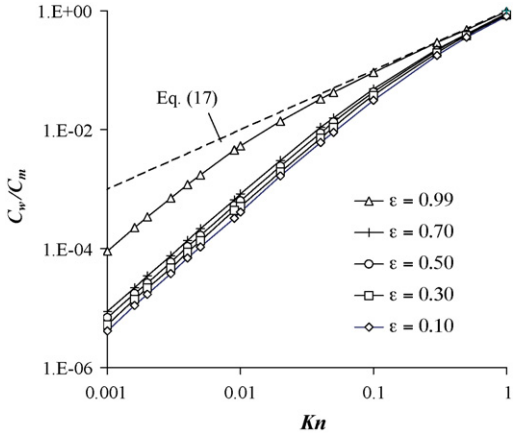

Fig. 12. Variation of the relative collision frequency with the Knudsen number at various porosities.

3.4. Insiders and stoppers

The only two types of tracks encountered in the molecular trajectories in diffusion controlled reaction systems are insiders and stoppers (since starters and crossers are only generated with reflection from the pore surface). The frequencies of insiders and stoppers are identically equal to those of intermolecular and molecule-wall collisions, respectively, in all types of diffusional flow. Therefore, the total length of molecular trajectories in diffusion controlled reaction processes may be obtained from $C_m l_i + C_w l_s$, as well as from $(C_m + C_w) l_a$, which gives readily

$$l_i = l_a + \frac{C_w}{C_m}(l_a - l_s) \tag{22}$$

At high values of the Knudsen number, insiders become increasingly scarce, therefore $l_a \to l_s$ and Eq. (21) predicts $l_i \cong l_a$ (i.e., $l_i \cong l_a \cong l_s$, in agreement with Eq. (18)). At low values of Kn, the relative collision frequency, C_w/C_m, attains very small values (Fig. 12), hence Eq. (22) predicts again $l_i \cong l_a$. In other words, the average length of insiders is predicted to remain practically equal to the overall average track length in both the bulk and Knudsen regime. Our simulation results are indeed in very good agreement with these predictions: In the bulk regime, the average value of the ratio l_a/l_i is found equal to 1.002 at Kn = 0.02 and 1.0004 at Kn = 0.01. In the transition regime, its value increases slightly up to a maximum of 1.032 at Kn = 1, then falls gradually back to 0.998 in the Knudsen regime, as predicted by Eq. (22).

The average length of stoppers in diffusion controlled reaction systems may also be obtained from Eq. (22), written in the form $l_s = l_a + (l_a - l_i)/(C_w/C_m)$. Nonetheless, since both $l_a - l_i$ and C_w/C_m approach zero asymptotically as Kn → 0, their ratio becomes indeterminate at that limit, thus preventing a straightforward prediction of the corresponding value of l_s. That limiting value is obtained from our simulations in dimensionless form as $\frac{l_s}{\bar{\lambda}} \cong 1.5$, as also shown in Table 3, where the average length of stoppers is compared to the overall average track length for various values of Kn, separately for $\varepsilon \leq 0.7$ and $\varepsilon = 0.99$ (no significant or systematic variation of l_s with ε is encountered for $\varepsilon \leq 0.7$). The above-claimed trend $l_a \to l_s$ for Kn → ∞ is indeed observed in the data shown in this table. However, at lower val-

Table 3
Comparison of the average length of stoppers to the overall average track length

Kn	$\varepsilon \leq 0.70$		$\varepsilon = 0.99$	
	$\left\langle \frac{l_a}{\bar{\lambda}} \right\rangle$	$\left\langle \frac{l_s}{\bar{\lambda}} \right\rangle$	$\frac{l_a}{\bar{\lambda}}$	$\frac{l_s}{\bar{\lambda}}$
100	0.0099	0.0099	0.0099	0.0099
10	0.092	0.092	0.091	0.091
1	0.53	0.55	0.50	0.51
0.1	0.96	1.23	0.91	0.97
0.01	1.00	1.48	0.99	1.20
0.001	1.00	1.51	1.00	1.43

ues of Kn (i.e., for Kn < 1), the value of l_s becomes progressively higher than that of l_a, by as much as 50% at Kn = 0.001 and $\varepsilon \leq 0.7$. The significant deviation of this result from the predictions of Eq. (18) may once again be attributed to the absence of molecular reflections from the pore surface in diffusion controlled reaction trajectories. Such reflections would lead to a higher number of intermolecular and molecule-wall collisions in the proximity of the pore surface in the bulk and lower transition regime, and consequently to a higher number of stoppers of relatively small size, especially in small voids of the pore structure, thereby reducing l_s to the value predicted by Eq. (18). The deviation is less pronounced at $\varepsilon = 0.99$, where the probability of encountering small stoppers after reflections from the wall is considerably smaller, due to the rarity of small voids in such dilute fiber structures.

4. Summary and remarks

Computer simulation results were derived for the diffusion controlled reaction rate coefficient, molecular survival probability, average track length and relative collision frequency in the bulk, transition and Knudsen diffusion regime, in random fiber structures. The investigated porous media consist of cylindrical fibers allowed to overlap freely with their axes positioned and oriented randomly in the three-dimensional space. The numerical results were obtained from a discrete random walk mechanism simulating the molecular trajectories for various values of the porosity and Knudsen number. Theoretical predictions were derived for the Knudsen regime survival probability and diffusion controlled reaction rate constant from earlier probabilistic relations centered on the chord length distribution function.

The computed values of the survival probability were found to depend strongly on the porosity and Knudsen number. Higher values were obtained at higher porosities, i.e., fewer molecules were found to collide with the pore wall in more dilute structures, for the same diffusion time. On the other hand, lower values of the survival probability were encountered at higher Knudsen numbers for a constant diffusion time, i.e., more molecules were found to collide with the wall by a certain time when fewer molecules were present in the pore volume, as anticipated by intuition. Higher values of the dimensionless mean survival distance were obtained in the bulk regime due to the significantly higher number of intermolecular collisions associated with this type of diffusion. The numerical results for the survival probability distribution and mean survival distance in the Knudsen regime practically coincide with analytical predictions for that type of diffusion. The employed number of random walkers was found to be high enough to provide accurate and reproducible values of the survival probability density, for all practical purposes.

The dimensionless diffusion controlled reaction rate coefficient remains practically constant in the bulk regime, with its value obeying an upper bound of the literature throughout the porosity range. At the other end of the diffusion spectrum, its value is in line with our analytical predictions, whereas in the transition regime it depends strongly on the Knudsen number. A harmonic average approximation based on Bosanquet's equation for the effective diffusivities is found to predict successfully the value of the diffusion controlled reaction rate coefficient in the transition regime from those in the bulk and Knudsen regimes.

Our numerical results for the average track length, average length of distinct types of tracks, and relative frequency of intermolecular and molecule-wall collisions in diffusion controlled reaction processes in random fiber structures deviate in general from earlier analytical predictions and simulation results for mass transfer by diffusion in the same type of porous media. The deviations are encountered in the biggest part of the transition regime, for all but the highest porosities, but vanish in the upper transition and Knudsen regime, at all porosity levels. This behavior is readily interpreted through an analysis centered on the basic differences of molecular trajectories in diffusion controlled reaction systems from those involving molecular reflection from the pore surface.

To our knowledge, this is the first numerical investigation of the diffusion controlled reaction rate coefficient and related parameters in the transition regime for any type of porous medium and in the Knudsen regime for any type of fiber structure. This study examined the case of perfectly absorbing walls (instantaneous surface reaction), characterized by a negligible frequency of molecular reflection from the pore surface. Random walk algorithms could be developed to extend the investigation to systems where the effective reaction rate is controlled by both diffusion and surface reaction kinetics.

References

[1] M.M. Tomadakis, S.V. Sotirchos, AIChE J. 39 (1993) 397.
[2] M.M. Tomadakis, S.V. Sotirchos, J. Chem. Phys. 99 (1993) 9820.
[3] M.M. Tomadakis, S.V. Sotirchos, Chem. Eng. Sci. 48 (1993) 3323.
[4] S. Borrelli, M. Giordano, P. Salatino, Chem. Eng. J. 64 (1996) 77.
[5] S.-Y. Lin, Y. Suzuki, H. Hatano, K. Tsuchiya, Chem. Eng. Sci. 55 (2000) 43.
[6] J.B. Chung, J.S. Chung, Chem. Eng. Sci. 60 (2005) 1515.
[7] M. Bizzi, L. Basini, G. Saracco, V. Specchia, Chem. Eng. J. 90 (2002) 97.
[8] R. Naslain, A. Guette, F. Rebillat, S. LeGallet, F. Lamouroux, L. Filipuzzi, C. Louchet, J. Mater. Sci. 39 (2004) 7303.
[9] W. Strieder, Chem. Eng. Sci. 55 (2000) 2579.
[10] P.M. Richards, J. Chem. Phys. (1986) 3520.
[11] H.P.G. Drewry, N.A. Seaton, AIChE J. 41 (1995) 880.
[12] C.A. Miller, I.C. Kim, S. Torquato, J. Chem. Phys. 94 (1991) 5592.
[13] L.H. Zheng, Y.C. Chiew, J. Chem. Phys. 90 (1989) 322.
[14] S. Torquato, I.C. Kim, J. Appl. Phys. 72 (1992) 2612.
[15] S. Torquato, Phys. Rev. Lett. 64 (1990) 2644.
[16] M.M. Tomadakis, T.J. Robertson, J. Chem. Phys. 122 (2005) 579.
[17] M.M. Tomadakis, T.J. Robertson, J. Compos. Mater. 39 (2005) 163.
[18] P. Levitz, Mater. Res. Soc. Symp. Proc. 290 (1993) 197.
[19] M.M. Tomadakis, S.V. Sotirchos, Radiat. Res. 135 (1993) 302.
[20] R.S. Caswell, Radiat. Res. 27 (1966) 92.
[21] A.M. Kellerer, Radiat. Res. 47 (1971) 359.
[22] R. Coleman, J. Appl. Probab. 6 (1969) 430.
[23] M.M. Tomadakis, S.V. Sotirchos, AIChE J. 37 (1991) 74.
[24] S. Whitaker, The Method of Volume Averaging, Kluwer Academic Publishers, 1999.
[25] W.G. Pollard, R.D. Present, Phys. Rev. 73 (1948) 762.
[26] M.M. Tomadakis, T.J. Robertson, J. Chem. Phys. 119 (2003) 1741.
[27] S. Prager, Chem. Eng. Sci. 18 (1963) 227.
[28] W. Strieder, J. Chem. Phys. 112 (2000) 2967.